Environmental Science & Technology

pubs.acs.org/est

Article

Machine Learning Models of Groundwater Arsenic Spatial Distribution in Bangladesh: Influence of Holocene Sediment Depositional History

Zhen Tan, Qiang Yang, and Yan Zheng*

Cite This: Environ. Sci. Technol. 2020, 54, 9454−9463

Read Online

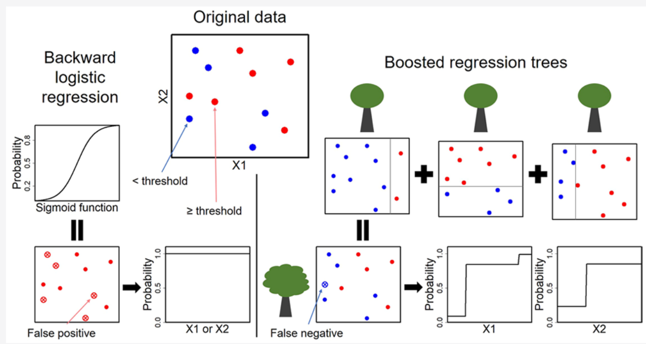

ABSTRACT: Recent advances in machine learning methods offer the opportunity to improve risk assessment and to decipher factors influencing the spatial variability of groundwater arsenic ($[As]_{gw}$). A systematic comparison reveals that boosted regression trees (BRT) and random forest (RF) outperform logistic regression. The probability of $[As]_{gw}$ exceeding 5 μg/L (approximate median value of Bangladesh $[As]_{gw}$), 10 μg/L (WHO provisional guideline value), and 50 μg/L (Bangladesh drinking water standard) is modeled by BRT and RF methods for Bangladesh and its four subregions demarcated by major rivers. Of the 109 geo-environmental and hydrochemical predictor variables, phosphorus and iron emerge as the most important across spatial scales, consistent with known As mobilization mechanisms. Well depth is significant only when hydrochemical parameters are not considered, consistent with prior studies. A peak of probability of $[As]_{gw}$ exceedance at ~30 m depth is evident in the partial dependence plots (PDPs) for spatial-parameter-only models but not in the equivalent all-parameter models, suggesting that sediment depositional history explains interdependent spatial patterns of groundwater As−P−Fe in Holocene aquifers. The South region exhibits a decrease of probability of $[As]_{gw}$ exceedance below 150 m depth in PDPs for spatial-parameter-only and all-parameter models, supporting that the deeper Pleistocene aquifer is a low-As water resource.

■ INTRODUCTION

A common yet unexplained characteristic of groundwater arsenic ($[As]_{gw}$) spatial distribution is the extensive variability at various spatial scales, as evidenced by local scale studies[1,2] with higher sampling densities ($\geq 10^{-1}$ per km^2) and basin scale studies[3−5] with lower sampling densities ($\leq 10^{-2}$ per km^2). Understanding what factors influence the spatial variability across spatial scales[6,7] is of interest because elevated concentrations of geogenic As in groundwater at levels above 10 μg/L, the World Health Organization's (WHO) provisional guideline value for drinking water, have been detected in more than 70 countries,[8] with up to 220 million people at risk of exposure based on a machine learning model.[9] Chronic exposure to drinking water As, a known carcinogen, is associated with a range of cancer and noncancer health outcomes.[10,11] Bangladesh where an estimated 45 million people are exposed to >10 μg/L As is facing a severe human health toll of an arsenic-related mortality rate of 1 in every 18 adult deaths.[12,13]

Logistic regression (LR) has been frequently used to model the spatial distribution of probability of $[As]_{gw}$ exceedance and to estimate the population at risk of exposure to elevated As in groundwater at global[14] and regional scales (10^5−10^8 km^2) across New England,[15] Southeast Asia[16] including Pakistan[17] and Vietnam,[18] China,[19] and continental United States,[20] as well as at smaller scales (10^3−10^4 km^2) for central Maine,[21] South Louisiana,[22] and the Central Valley of California,[23] (Table S5). An LR model in Southeast Asia including Bangladesh[16] also illustrated the association between As occurrence and Holocene deltaic and organic-rich deposits. This apparent association is believed to be driven by sluggish flow and reducing conditions favoring As mobilization in such aquifers[6,24] at regional scales, although at local scales mechanisms of As mobilization could involve pyrite oxidation.[25,26] Further, inclusion of hydrogeochemical parameters to LR models has been shown to not only improve the model performance in central Maine[21] but also to offer insights into common drivers that are important explanatory variables

Received: June 4, 2020
Revised: July 9, 2020
Accepted: July 10, 2020
Published: July 10, 2020

https://dx.doi.org/10.1021/acs.est.0c03617
Environ. Sci. Technol. 2020, 54, 9454−9463

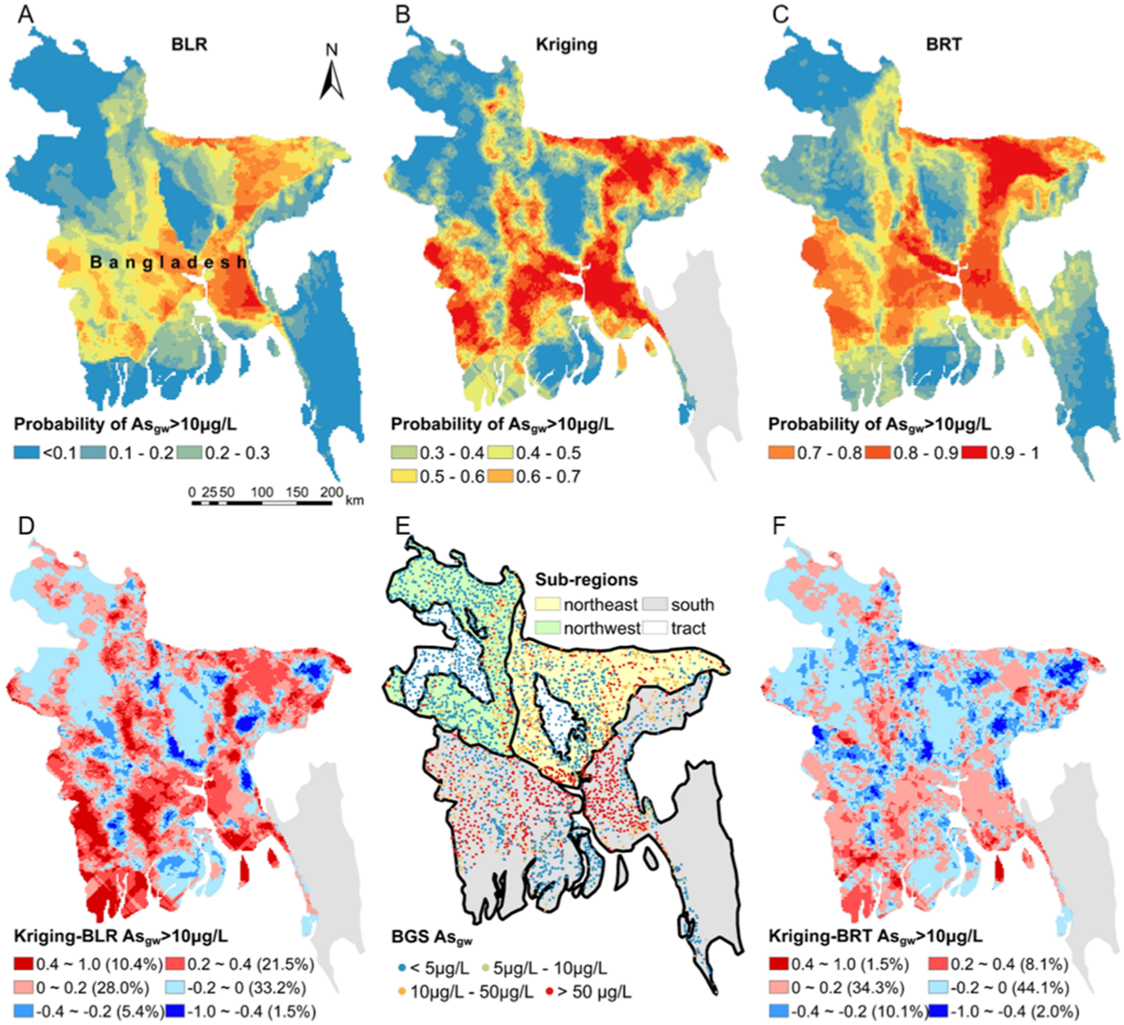

Figure 1. Probability of groundwater arsenic concentration ($[As]_{gw}$) exceeding the WHO provisional guideline value for arsenic in drinking water of 10 μg/L in Bangladesh obtained by (A) backward logistic regression (BLR), (B) kriging, and (C) boosted regression trees (BRT). The difference between the probability based on the BLR spatial-parameter-only model prediction (A) and kriging (B) is shown in (D), while that between kriging (B) and the BRT spatial-parameter-only model prediction (C) is shown in (F). (E) Map of $[As]_{gw}$ of 3538 wells in Bangladesh surveyed by BGS and DPHE (2001)[4]. The blue, green, yellow, and red dots represent $[As]_{gw}$ $\leq$5 μg/L, 5−10 μg/L, 10−50 μg/L, and >50 μg/L, respectively. The data-sparse Chittagong Hill tract in SE Bangladesh has been excluded from kriging (B) and thus comparison with models (D) and (F).

for the spatial patterns of groundwater arsenic and its mobilization.

Although the linkage between geo-environmental parameters used as predictor variables and $[As]_{gw}$ can be captured[21,27] by the LR models, the model performance is often less than satisfactory due to the coarse spatial resolution of most parameters.[15,20] Logistic regression also has a weakness in the assumption of independence of all explanatory variables, which in reality are often correlated.[16−18,20] Among prior studies that have employed traditional methods such as correlation analysis, linear regression, and generalized linear regression, poor model performance is also common.[28−30] Novel weak-learner ensemble regression tree models utilized in ecology studies[31,32] have shown less influence by the parameter multicollinearity and demonstrated improved model performance.[9] A recent boosted-tree model has resulted in improvements for modeling groundwater As distribution in the Central Valley.[23] However, research is needed to understand the reason for this improvement through a systematic comparison of methods. Only a few studies have attempted to characterize the still enigmatic spatial patterns of groundwater As at various spatial scales (10^{-1}−10^{8} km^2) through statistical spatial models.[33,34] A classification and regression tree (CART) analysis of 40 215 data points of groundwater As and 30 additional chemical parameters has identified aridity, pH, iron, and phosphate as significant controlling factors for groundwater arsenic at national and regional scales in the United States.[35] Much remains to be done to elucidate factors regulating spatial patterns of groundwater As.

Given the potential advantages of machine learning methods and that hydrochemical parameters have not previously been considered in LR models for As in Bangladesh, this study set out first to systematically compare the performance of a traditional method backward logistic regression (BLR) with those of machine learning methods (BRT and RF) to determine which method is better suited for risk assessment. Second, spatial-parameter-only models (including all geo-environmental parameters but excluding hydrogeochemical parameters) and all-parameter machine learning models are constructed for both national and regional scales of Bangladesh

https://dx.doi.org/10.1021/acs.est.0c03617
Environ. Sci. Technol. 2020, 54, 9454−9463

Table 1. Descriptive Statistics of Groundwater Arsenic Concentration in Bangladesh and Five Regions Reported by BGS and DPHE, 2001, and the Relative Importance Scores of the Top Two-Ranked Parameters in All-Parameter and Spatial-Parameter-Only BRT Models

region	number of samples	area (km^2)	$[As]_{gw}$median (μg/L)	$[As]_{gw}$mean (μg/L)	$[As]_{gw}$max (μg/L)	percentage of samples >5 μg/L (%)	percentage of samples >10 μg/L (%)	percentage of samples >50 μg/L (%)	rel. importance score BRT all-models[a]	rel. importance score BRT spatial models[b]
Nation	3538	147 570	3.8	55.0	1660	47.9	42.1	24.9	P (100), Fe (65)	depth (100), Dis2Meg (77)
South	1567	78 676	16.0	94.4	1660	59.9	54.6	39.2	Fe (100), depth (30)	depth (100), I-B ranges (25)
South-Shallow (<150 m)	1259	78 676	47.1	118.8	1660	72.4	67.1	48.7	P (100), Fe (42)	I-B ranges (100), Dis2Meg (77)
Northeast	858	29 884	11.6	39.5	573	63.7	55.4	25.3	P (100), Fe (42)	Dis2Bra (100), depth (80)
Northwest	796	26 282	1.0	15.5	708	27.5	21.9	7.5	Fe (100), P (50)	Dis2Bra (100), depth (47)
Tract[c]	317	12 728	<0.5	1.0	21.2	4.4	1.3	0.0		

[a]The relative importance score is relative to the highest ranked parameter, with its value set to 100. Here, only >10 μg/L threshold modeling results are listed with the rest in Tables S7 and 8. [b]Dis2Meg, Dis2Bra, and I-B ranges are the distance to the Meghna river, the distance to the Brahmaputra river, and the Indo-Burman ranges, respectively. [c]Tract areas are not modeled due to a low $[As]_{gw}$ exceedance rate. The minimum $[As]_{gw}$ for all areas is <0.5 μg/L.

with respect to three As thresholds of 5, 10, and 50 μg/L. Comparison of controlling factors including hydrogeochemical processes across scales improves confidence in underlying mechanisms for As spatial distribution, with implications for As mitigation policy. Finally, interpretation of the modeling results builds on a new understanding of Holocene sediment depositional history to illustrate its influence on groundwater As spatial patterns in Bangladesh. Because of the worldwide occurrence of geogenic As in groundwater,[8] the finding has implications for improving risk assessments through machine learning and understanding of As mobilization in aquifers with similar hydrogeological settings.[9]

MATERIALS AND METHODS

Arsenic Data. The groundwater hydrochemical dataset (n = 3,538) with 20 parameters including well depth, concentration of groundwater As ($[As]_{gw}$, Figure 1), iron (Fe), and phosphorus (P) was obtained ca. 2000.[4] Measured $[As]_{gw}$ was converted to binary $[As]_{gw}$ exceedance using threshold values of 5 μg/L (similar to the Bangladesh $[As]_{gw}$ median of 3.8 μg/L, Table 1), 10 μg/L (WHO provisional guideline value), and 50 μg/L (Bangladesh drinking water standard), respectively, and used as the dependent variable for further analysis and modeling. The national dataset was divided into four subdatasets for four regions (Figure 1) demarcated by three major rivers (Brahmaputra, Ganges, and Meghna): the South (n = 1567, median $[As]_{gw}$ 16.0 μg/L), Northeast (n = 796, median $[As]_{gw}$ 11.6 μg/L), Northwest (n = 858, median $[As]_{gw}$ 1.0 μg/L), and the Barind and Madhupur Tracts (n = 317, median $[As]_{gw}$ <0.5 μg/L) (Table 1). In the uplifted Pleistocene Barind and Madhupur Tracts,[30] $[As]_{gw}$ was >5 μg/L in 4% of samples, with 1% >10 μg/L. Therefore, the data from the Tracts were not analyzed further. A South-Shallow dataset (n = 1259, median $[As]_{gw}$ 47.1 μg/L), a subset of the South regional dataset but consisted only of wells with depth <150 m,[36,37] was also analyzed. The distribution of As is skewed, with the percentage of samples above three thresholds decreasing from the South-Shallow and the Northeast to the Northwest (Table 1). The percentage of samples of $[P]_{gw}$ >0.8 mg/L (Table S2a) and of $[Fe]_{gw}$ >1.2 mg/L (Table S2b) also followed this order.

Kriging. Probability kriging (Geostatistical Analyst in ArcGIS 10.5)[38] was applied to the BGS and DPHE dataset to interpolate the probability of As exceeding the three thresholds of 5, 10, and 50 μg/L (Figure S5). Probability kriging (Supporting Information (SI) Text S4) considers spatial autocorrelation of groundwater As and cross-correlation with other variables.[39] Prior studies using the same dataset[4,33] have shown that the kriged As distribution was able to capture the spatial variation at 3−150 km scales. Therefore, the kriged probability map was used as a benchmark to compare with maps from machine learning model predictions (Figure 1).

Predictor Variables. A total of 90 geo-environmental spatial parameters that encompass topography, soil, climate, and geology factors available at various spatial resolution (Table S1) are used as predictor variables in the spatial-parameter-only models. These geo-environmental spatial parameters were chosen to represent multifaceted processes that might affect As mobilization and to include parameters (n = 30) of a prior LR model.[16] All-parameter models used a total of 109 parameters, adding 19 hydrochemical parameters from the BGS and DPHE dataset to 90 spatial parameters.

Comparison of Logistic Regression and Machine Learning Methods. National all-parameter models for the threshold level of 10 μg/L were constructed specifically to compare methods (Figure S1). The dataset was randomly split into training and testing sets at a ratio of 7:3 while maintaining the same $[As]_{gw}$ exceedance rates, and this was repeated 1000 times for BLR, BRT, and RF model runs. A stepwise backward method of LR (BLR) is implemented similar to a prior LR model[16] but started with an expanded and updated set of 109 parameters. The glm and step function[40] were used, with one parameter removed each step (stepwise) to reach the minimum Akaike's information criterion value (AIC, an estimate of the quality of a model relative to other models). BRT and RF methods are described later. A probability cutoff (or cut point) of 0.50 is used. Prior studies have evaluated cutoffs of 0.2 and 0.5 for continental USA[20] as well as the statistically determined cutoffs of 0.57 and 0.72 for a global model,[9] with the low cutoff of 0.2 resulting in too many false positives and the high cutoff of 0.72 resulting in too many false negatives.

https://dx.doi.org/10.1021/acs.est.0c03617
Environ. Sci. Technol. 2020, 54, 9454−9463

Because the ensemble tree models (BRT and RF) do not make assumptions of data distribution or independency like the BLR, they have been shown to capture the interaction of parameters with stronger performance on datasets with multiple parameters.[31,41] To verify this, the performance of each method was evaluated via four comparison statistical measures, accuracy, sensitivity, specificity, and the area under the curve (AUC) of receiver operator characteristics (ROC). There are true positives (TP), true negatives (TN), false positives (FP), and false negatives (FN) in the predictions. Accuracy is the proportion of true prediction or TP/(TP + FP). Sensitivity is TP/(TP + FN), while specificity is TN/(TN + FP). Created by plotting the true positive rate (sensitivity) against the false positive rate (1-specificity), the AUC of ROC evaluates the ability to distinguish classes above or below certain thresholds.

Machine Learning Models. A total of 112 models, 56 boosted regression trees (BRT)[42] and 56 random forest (RF) models, using 5, 10, and 50 μg/L thresholds were constructed for the national and four regional datasets, respectively (Figure S1). All datasets were again randomly split into training and testing sets at a ratio of 7:3. The BRT models in booting decision trees were built in a stagewise fashion, starting with a single tree fitting for the entire training dataset, and then generating new trees serially along the steepest descent to improve the model accuracy in each loop.[43] In RF bagging decision tree models, each tree was generated concurrently and independently to fit a random bootstrap-resampling set of training data with a random subset of the parameters, followed by combining the trees by majority to give a representative output of all individual trees.[44] The GBM[45] and random Forest[46] packages in R were used for the BRT and RF models, respectively.

A 10 times repeated 10-fold cross-validation (CV) was used to tune BRT and RF models using the AUC of ROC. For BRT models, all four hyperparameters were tuned for 9 models (see the SI for details). This tuning exercise found that if two boosting structure hyperparameters n.trees and shrinkage are set to 1000 and 0.005, respectively, tuning the other two hyperparameters can achieve excellent and comparable performance. Thus, only interaction.depth (the maximum depth of variable interactions, 10, 15, 20, and 25) and n.minobsinode (the minimum number of observations in terminal nodes, 10, 15, 20, 25, and 30) were tuned for all 56 BRT models. For 56 RF models, mtry (number of variables randomly subsampled, 5−20) was tuned. The caret[47] package was utilized for tuning.

Partial Dependence Plot (PDP). The PDP is used to show the marginal effect that one or two features have on the predicted outcome of a machine learning model.[43] Here, the predicted outcome is the probability of As exceedance and the features are the predictor variables with high importance scores: Fe, P, and depth. Comparisons of PDPs of all-parameter and spatial-parameter-only BRT models are used to infer hydrochemical and sediment depositional processes controlling $[As]_{gw}$ spatial patterns across scales.

Importance Score. To identify the controlling factors for $[As]_{gw}$ spatial patterns across scales, the importance score was calculated for the three thresholds in national and regional models. For each predictor variable, the relative importance score normalized to the highest scored parameter assigned to a value of 100 is reported (Tables S7 and S8). Classification models tend to overvalue the fitting accuracy of the majority class. Therefore, preprocessing of the training dataset to reduce its skewness,[48] or oversampling (see the SI for details), has been applied in 26 BRT and 26 RF models solely to calculate the importance score (Figure S1).

RESULTS AND DISCUSSION

BRT and RF Are Better than BLR for Modeling Bangladesh Groundwater As. Unlike data in other scientific disciplines, geoscience data are frequently spatial with autocorrelation and tend to form spatial clusters.[49] Predictive models based on spatial data are more sensitive to the partition of training and testing datasets[50] and tend to have significant variances due to either low data density or uneven distribution. But systematic evaluation of the effect of potentially large variances in random splitting of training and testing datasets is lacking and is hence attempted here. A prior LR model for Bangladesh[16] displayed a training accuracy of 70% and a testing accuracy of 63%. Here, the accuracy, sensitivity, specificity, and AUC of ROC of the ensemble tree methods RF and BRT applied in all-parameter and spatial-parameter-only national models outperformed similarly constructed BLR models (Figure 2). These four measures of model performance were also more variable for BLR than those of RF and BRT (Figure 2).

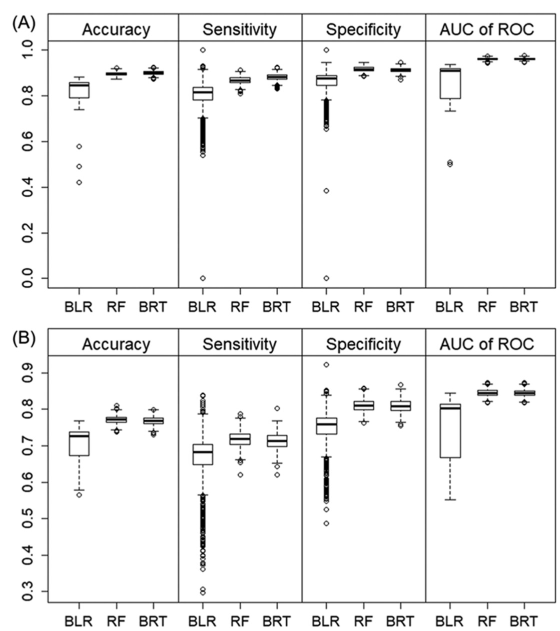

Figure 2. Four statistic measures, accuracy, sensitivity, specificity, and the area under curve (AUC) of the receiver operator characteristics (ROC) are shown from left to right to compare the performance of the BLR, RF, and BRT methods for modeling the probability of $[As]_{gw} > 10$ μg/L with a 70−30% split in training and testing sets and 1000 random stratified partitions for (A) all-parameter models and (B) spatial-parameter-only models.

Improved Risk Assessment in Bangladesh by BRT Spatial-Parameter-Only Models. The kriging interpolated map of Bangladesh $[As]_{gw}$ is only meaningful at regional and national scales but not at local scales (<3 km) because the variogram barely changes for distances less than 3 km.[4,33] Compared with the kriging map of probability of $[As]_{gw}$ exceeding 10 μg/L, the BRT spatial-parameter-only model-predicted map (see SI Text S5) has more evenly distributed

https://dx.doi.org/10.1021/acs.est.0c03617
Environ. Sci. Technol. 2020, 54, 9454−9463

under- or overestimations in smaller magnitude, while the BLR-predicted map underestimates the exceedance probability for many parts of Bangladesh (Figure 1). The most notable improvement of the BRT-predicted probability lies in southwestern Bangladesh and parts of northeastern Bangladesh when compared with the BLR method (Figure 1). The RF spatial-parameter-only model-predicted maps of $[As]_{gw}$ exceeding 5, 10, and 50 μg/L are similar to those by BRT (Figure S5). Such improved risk assessment maps are consistent with the superior performance of machine learning methods over logistic regression (Figure 2). Because the $[As]_{gw}$ dataset (Table 1) has a high degree of skewness of 3.76, BRT displays comparable specificity but better testing sensitivity than RF for most national and regional models across scales (Table S6 and Figure S10).

Whenever possible, predictive models are recommended for $[As]_{gw}$ risk assessment to complement interpolation-based methods. Because the "true" $[As]_{gw}$ distribution and the mechanisms for the spatial patterns remain elusive across spatial scales, multiple approaches are warranted to improve confidence. Model-generated maps consider interactions of multiple parameters, so a comparison of assessments from interpolation such as kriging and from models can shed light on the underlying mechanisms—this is discussed later. Yu et al.[33] have examined the changes in the variance of the variogram in the same BGS and DPHE[4] dataset by subdividing the entire Bangladesh to 34 geologic−geomorphic regions and detrending of depth. They demonstrate that the spatial variance of $[As]_{gw}$ depends on the geologic−geomorphic unit and depth. This is what has motivated this study to construct models at regional scales to take advantage of this critical understanding, which has not previously been considered in the risk assessment modeling of Bangladesh.

Risk assessment of As concentrations is also helpful but not attempted here. Artificial neural network (ANN) and support vector machine (SVM) methods have been used to predict As concentration,[51−53] as well as to predict the probability of $[As]_{gw}$ exceedance.[54] However, these methods require high data density because low data density leads to underfitting or aggravates overfitting.[52,53]

Importance of Well Depth across Scales Based on Spatial-Parameter-Only Models. In BRT and RF spatial-parameter-only models, well depth emerged as the parameter with the highest importance score at national and most regional scales (Figure 3), and the distance to one of the major rivers usually was another parameter ranked among the top two in models across scales (Tables 1 and S8).

The PDPs showed the marginal effects of the influence of important parameters on the estimation of the probability of $[As]_{gw}$ exceedance. The PDPs of well depth for the South region resembled that of the entire Bangladesh, with a large decrease at 150 m (Figure 3A,C), consistent with the well-known depth trend of $[As]_{gw}$.[4] This highlights 150 m as an important depth control of $[As]_{gw}$ in southern Bangladesh where 308 or ∼20% of wells out of 1567 wells are from >150 m depth (Table 1). The 30 m local maximum of the probability of $[As]_{gw}$ exceedance was evident in regional spatial-parameter-only models for the South-shallow and the Northeast but not the Northwest (Figure 3C), suggesting that the 30 m local maximum in the three national models (Figure 3A) reflects features mostly in the South and the Northeast regions that consist of Holocene fluvial and deltaic aquifers.

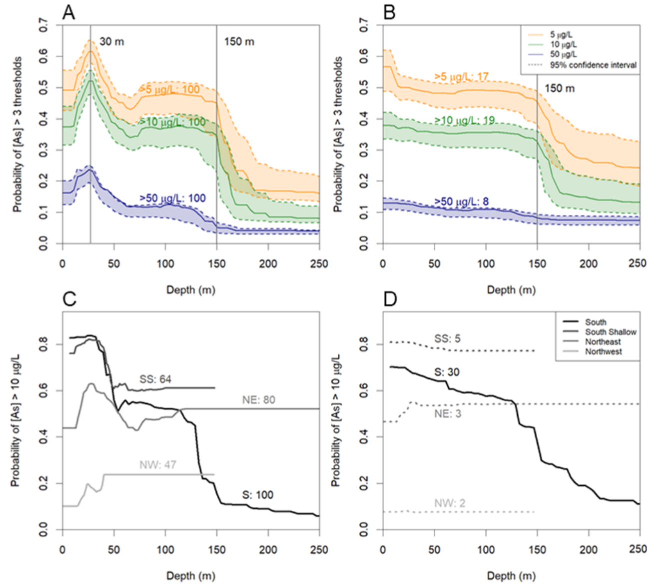

Figure 3. Partial dependence plots (PDPs) of well depth in the BRT national models of spatial-parameter-only (A) and all-parameters (B), with respect to thresholds of 5 μg/L (orange line), 10 μg/L (green line), and 50 μg/L (blue line). The same colored envelope between the dashed lines indicates the 95% confidence interval. The PDPs of well depth in the BRT regional (S: South, SS: South-Shallow, NE: Northeast, and NW: Northwest) models of spatial-parameter-only (C) and all-parameters (D), with respect to the threshold of 10 μg/L. In all panels, the relative importance scores of well depth are written next to the line in the same color, with the gray dashed line in (D) representing very low scores except for the South region (solid line).

Regional depth profiles of $[As]_{gw}$ and exceedance probability (Figure S2) support the features in PDPs.

All-Parameter Models Reveal that P and Fe Influence As Spatial Distribution across Scales. In BRT and RF all-parameter models, groundwater phosphorus and iron are consistently scored as the two most important across most scales except for the South region (Table 1 and Figure 4). In BRT all-parameter models at the national scale (Figure 4A), groundwater P scored 100 or the highest importance. The relative importance score of groundwater Fe was second only to P and was 77, 65, and 19 in the same BRT all-parameter models at the national scale for the probability of $[As]_{gw}$ exceeding 5, 10, and 50 μg/L, respectively (Figure 4B). In these models with hydrochemical parameters, the relative importance of well depth ranked far below P and Fe, except for the South where it ranked second (Figure 3D).

The PDPs of national all-parameter models show that the probability of $[As]_{gw}$ exceeding 10 μg/L increases with P until it reaches 0.8 mg/L, after which the probability stabilizes at 0.79 (Figure 4A). For Fe, the probability of $[As]_{gw}$ exceeding 10 μg/L increases with Fe until it reaches 1.2 mg/L, after which the probability stabilizes at 0.6 (Figure 4B). In most regional all-parameter models, P and Fe displayed PDPs similar to the national all-parameter models (Figure 4C,D), except for the Northwest region where the concentrations of groundwater P are substantially lower than those of other regions, but the concentrations of groundwater Fe are only somewhat lower than those of other regions (Table S2). In addition, Fe scored higher than P for the South and the Northwest regions (Table 1).

https://dx.doi.org/10.1021/acs.est.0c03617
Environ. Sci. Technol. 2020, 54, 9454−9463

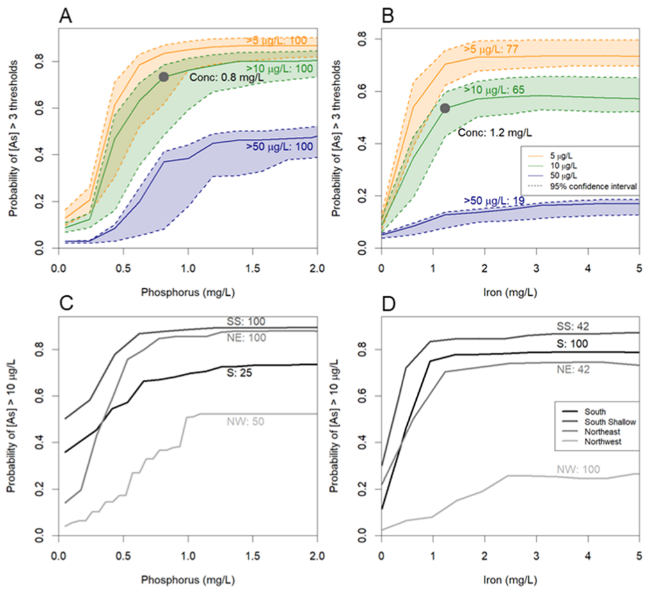

Figure 4. Partial dependence plots (PDPs) of phosphorus (A) and iron (B) in all-parameter national BRT models exceeding the $[As]_{gw}$ thresholds of 5 μg/L (orange line), 10 μg/L (green line), and 50 μg/L (blue line) with 95% confidence interval indicated by the same colored envelope between dashed lines. The PDPs of phosphorus (C) and iron (D) in the regional BRT all-parameter models of the South (S), South-Shallow (SS), Northeast (NE), and Northwest (NW) are only for the threshold of 10 μg/L. In all panels, the relative importance scores of iron or phosphorus are written next to the line in the same color.

CART analysis of the U.S. groundwater data has identified that dissolved iron (taken to represent chemically reducing conditions), pH, and phosphate (released also due to reductive dissolution of Fe/Mn-oxyhydroxides) were the top three statistically significant covariates in the temperate (eastern) region consisted of coastal aquifers.[35] This is a likely biogeochemical mechanism that also drives simultaneous Fe–As–P mobilization in Bangladesh aquifers. Of all predictor variables, only hydrochemical parameters were sampled at the exact same location as that of the groundwater As data, while the rest were generated from the extraction of raster data collected on usually coarser spatial resolution (Table S1). This might be why all-parameter models outperform spatial-parameter-only models (Table S6) because the spatial resolution of both dependent variable (i.e., $[As]_{gw}$) and predictor variables affects the performance. After inclusion of hydrochemical parameters to a BLR model using only geological parameters, an increase in testing accuracy from 57 to 76% in central Maine has also been found.[21]

Implications for As Mitigation Policy Relying on Deep Groundwater (>150 m). That our models consistently identified 150 m depth as an important control for the South region of Bangladesh lends support to the most widely adopted mitigation policy[55−57] for that region. Drilling wells to greater than 150 m depth has been a national policy since the release of the BGS and DPHE dataset in 2001.[4] The PDPs for both the national and the South regional spatial-parameter-only models (Figure 3A,C) and all-parameter models (Figure 3B,D) displayed a significant decline at 150 m depth, below which the probability of $[As]_{gw}$ exceeding 10 μg/L is between 10 and 20%. This "150 m" feature suggests a geologic or sediment stratigraphy control, supported by numerous studies over the past two decades. Sea-level lowstands during several glacial periods have subjected the sediment below 150 m of the Plio-Pleistocene age[29] to extensive flushing over time scales of $>10^5$ years, resulting in weathered sediments dominated by Fe oxide with little organic matter[58] and mobilizable As.[55,56] Further, the impermeable paleosol formed atop the aquifer sediment in the same period is protective of the Pleistocene aquifer with low $[As]_{gw}$ from the contaminated shallower aquifer.[36,59] Reconstruction of late Pleistocene strata from bore hole logs has identified red beds at shallower depths of <100 m from the northern end of the South region (Dhaka) to patchy Pleistocene red beds at a depth of <100 m to possibly more extensive and likely continuous Pleistocene red beds at a depth of ∼150 m near the Sundarbans and the coast.[36,60] This depth trend follows the paleosol surface during the glacial lowstand.[59,61,62]

However, the PDPs do not identify any depth below which the probability of encountering elevated $[As]_{gw}$ is significantly reduced for the Northeast Sylhet Basin region (Figure 3C,D) because subsidence has allowed for rapid sediment accumulation since mid-Holocene.[63] This negates deep well installation as a mitigation policy in the Northeast.

Common Hydrogeochemical Processes Releasing P and Fe Are Key to Elevated Risks of As at 30 m Depth. The modeling results highlight that the elevated As risks at 30 m depth and the associated hydrogeochemical mechanisms mobilizing P and Fe are common in the Holocene aquifers of the South-Shallow and the Northeast regions. This is based on the contrasting PDPs of the South-Shallow and the Northeast regions: the 30 m local maxima of As exceedance are prominent in the spatial-parameter-only models (Figure 3C) but are missing in the equivalent all-parameter models (Figure 3D). The elevated risks of As around 30 m depth are consistent with the depth profiles (Figure S2) and mechanisms of As, P, and Fe mobilization established by detailed hydrochemical studies.[4,64−66] Probability in exceedance of 10 μg/L is >50% at ∼30 m depth based on the same BGS and DPHE dataset.[7] Microbial reduction of iron oxyhydroxides has been invoked as the mechanism responsible for As mobilization in reducing aquifers of Bangladesh.[67−70] Concentrations of P and As reflect to some extent the cumulative effect of the respiration of organic carbon associated fine-grained sediment rich in sorbed P and As[7,71] in aquifers with sluggish flow.[68,69] The analogous As and P chemical behavior[72−74] is also reflected in their similarities in the spatial and temporal variations in groundwater of Bangladesh Holocene aquifers.[75,76]

Role of Holocene Sediment Depositional History. Recent advances in the Holocene sediment depositional history of Bangladesh are supportive of the conditions conducive to the accumulation of organic-rich, fine-grained sediment with high As loading in the South and Northeast regions. First, a compilation of the radiocarbon ages of sediment organic carbon from bore holes in the South region[4,61,77] is used to calculate an average sedimentation rate of 391.5 cm/kyr (Figure S3). Using this rate, the sediment at 30 m depth would have been deposited around 6 ka BP, or during the Mid-Holocene Warm Period.[78,79] Second, a compilation of the available sediment chemistry data shows that labile As concentration ranged from 0.4 to 1.4 mg/kg in the fine-grained sediment of mid–late Holocene (depth 2–40 m), higher than 0.1 to 0.3 mg/kg in the sediment of early Holocene (Table S3). Taken together, the As–P spatial

https://dx.doi.org/10.1021/acs.est.0c03617
Environ. Sci. Technol. 2020, 54, 9454−9463

coupling, particularly the maximum occurrence of $[As]_{gw}$ at about 30 m depth in the South and Northeast regions, is likely through a common organic linkage due to a shift in the sediment depositional environment.

The significance of a mid-Holocene $[As]_{gw}$ peak is that it is found when profound shifts in the sedimentation environment toward deposition of finer, organic-rich sediments occurred, in association with a warmer climate then. Goodbred et al.[77] utilized sediment silicate Sr concentration together with Sr and Nd isotopes to reconstruct the history and interaction of the Ganges, Brahmaputra, and Meghna fluvial systems during Holocene. The monsoon weakening in mid-Holocene (6−4 ka BP) and progradation of the Brahmaputra in the Sylhet Basin of the Northeast decreases the sediment transport to the lower Ganges−Brahmaputra−Meghna delta,[77] resulting in transgression and eastward migration of the Ganges in the South/delta region[80] that formed the fine-grained and organic-rich sediment. To summarize, the progradation of the Brahmaputra in the Northeast/Sylhet region and the associated meandering of the Ganges in the South/delta region took place in mid-Holocene or ∼6 ka BP, with the sediment depositional environment switched from a coarse-grained channel-fill type to a fine-grained over-bank type, now found at a depth of ∼30 m.[77]

Limitations. That Fe is less important than P for the Holocene aquifer's As spatial pattern in the South and Northeast regions warrants further investigation. The biogeochemical reactions involving Fe and As in reducing aquifers do not necessarily support strong correlation between groundwater As and Fe concentrations,[81] with decoupling of As and Fe noted in studies of sedimentary profiles[82] and incubation experiments.[83] Iron-rich, sulfur-poor reducing groundwater also promotes siderite formation.[56,82] Transformation of iron minerals in the subsurface environment is complex,[24] with the newly formed mixed Fe(II)−Fe(III) minerals such as magnetite capable of sequestering As.[84] Iron is more important than P in the Northwest, possibly because the sediment there has a very different provenance, with a more dynamic depositional environment resulting in coarser grained, less organic-rich sediments. Groundwater arsenic in Bangladesh is geogenic in origin, with its spatial patterns (30 m depth As peak and >150 m low-As zone) controlled by sediment depositional and erosional histories coupled with climate history.

■ ASSOCIATED CONTENT

Supporting Information

The Supporting Information is available free of charge at https://pubs.acs.org/doi/10.1021/acs.est.0c03617.

> Framework of this study, depth profiles of As, Fe and P and descriptive statistics of Fe, P and depth; sediment accumulation pattern based on radiocarbon data compilation; kriging interpolation; mapping; tuning of hyperparameters in machine learning models; data preprocessing for importance score calculation; along with literature review of existing models and a compilation of radiocarbon ages; detailed results of performance of machine learning models, importance scores, and partial dependence plots (PDF)

■ AUTHOR INFORMATION

Corresponding Author

Yan Zheng − *Guangdong Provincial Key Laboratory of Soil and Groundwater Pollution Control, School of Environmental Science and Engineering and State Environmental Protection Key Laboratory of Integrated Surface Water-Groundwater Pollution Control, School of Environmental Science and Engineering, Southern University of Science and Technology, Shenzhen 518055, China;* orcid.org/0000-0001-5256-9395; Phone: +86 755 88018037; Email: yan.zheng@sustech.edu.cn

Authors

Zhen Tan − *College of Engineering, Peking University, Beijing 100871, China; Guangdong Provincial Key Laboratory of Soil and Groundwater Pollution Control, School of Environmental Science and Engineering and State Environmental Protection Key Laboratory of Integrated Surface Water-Groundwater Pollution Control, School of Environmental Science and Engineering, Southern University of Science and Technology, Shenzhen 518055, China*

Qiang Yang − *Lamont-Doherty Earth Observatory of Columbia University, Palisades, New York 10964, United States*

Complete contact information is available at: https://pubs.acs.org/10.1021/acs.est.0c03617

Notes

The authors declare no competing financial interest.

■ ACKNOWLEDGMENTS

Funding for this research was provided by the National Natural Science Foundation of China (Grant 41831279 and 41772265), the Strategic Priority Research Program of the Chinese Academy of Sciences (Grant XDA20060402), and the Shenzhen Science and Technology Innovation Commission (Grant KQJSCX20170728163124680). We thank Julian Koch, Benjamin Bostick, Yuqin Sun, and Jie Liu for valuable discussions. We thank four anonymous reviewers for their constructive comments.

■ REFERENCES

(1) van Geen, A.; Zheng, Y.; Versteeg, R.; Stute, M.; Horneman, A.; Dhar, R.; Steckler, M.; Gelman, A.; Small, C.; Ahsan, H.; et al. Spatial variability of arsenic in 6000 tube wells in a 25 km2 area of Bangladesh. *Water Resour. Res.* **2003**, *39*, 1140−1155.

(2) Yang, Q.; Jung, H. B.; Culbertson, C. W.; Marvinney, R. G.; Loiselle, M. C.; Locke, D. B.; Cheek, H.; Thibodeau, H.; Zheng, Y. Spatial pattern of groundwater arsenic occurrence and association with bedrock geology in greater Augusta, Maine. *Environ. Sci. Technol.* **2009**, *43*, 2714−2719.

(3) Berg, M.; Tran, H. C.; Nguyen, T. C.; Pham, H. V.; Schertenleib, R.; Giger, W. Arsenic Contamination of Groundwater and Drinking Water in Vietnam: A Human Health Threat. *Environ. Sci. Technol.* **2001**, *35*, 2621−2626.

(4) BGS, DPHE. Arsenic Contamination of Groundwater in Bangladesh. In *British Geological Survey Technical Report WC/00/19*; Kinniburgh, D. G.; Smedley, P. L., Eds.; British Geological Survey: Keyworth, 2001.

(5) Ryker, S. J. Mapping arsenic in groundwater. *Geotimes* **2001**, *46*, 34−36.

(6) Smedley, P. L.; Kinniburgh, D. G. A review of the source, behaviour and distribution of arsenic in natural waters. *Appl. Geochem.* **2002**, *17*, 517−568.

(7) Fendorf, S.; Michael, H. A.; van Geen, A. Spatial and Temporal Variations of Groundwater Arsenic in South and Southeast Asia. *Science* **2010**, *328*, 1123−1127.
(8) Ravenscroft, P.; Brammer, H.; Richards, K. *Arsenic Pollution: A Global Synthesis*; John Wiley & Sons, 2009; Vol. *28*.
(9) Podgorski, J.; Berg, M. Global threat of arsenic in groundwater. *Science* **2020**, *368*, 845−850.
(10) Council, N. R. *Critical Aspects of EPA's IRIS Assessment of Inorganic Arsenic: Interim Report*; National Academies Press, 2013.
(11) Zheng, Y. Global solutions to a silent poison. *Science* **2020**, *368*, 818−819.
(12) Nickson, R.; McArthur, J.; Burgess, W.; Ahmed, K. M.; Ravenscroft, P.; Rahman, M. Arsenic poisoning of Bangladesh groundwater. *Nature* **1998**, *395*, No. 338.
(13) Flanagan, S. V.; Johnston, R. B.; Zheng, Y. Arsenic in tube well water in Bangladesh: health and economic impacts and implications for arsenic mitigation. *Bull. W. H. O.* **2012**, *90*, 839−846.
(14) Amini, M.; Abbaspour, K. C.; Berg, M.; Winkel, L.; Hug, S. J.; Hoehn, E.; Yang, H.; Johnson, C. A. Statistical modeling of global geogenic arsenic contamination in groundwater. *Environ. Sci. Technol.* **2008**, *42*, 3669−3675.
(15) Ayotte, J. D.; Nolan, B. T.; Nuckols, J. R.; Cantor, K. P.; Robinson, G. R.; Dalsu, B.; Laura, H.; Margaret, K.; William, B.; Silverman, D. T.; et al. Modeling the probability of arsenic in groundwater in New England as a tool for exposure assessment. *Environ. Sci. Technol.* **2006**, *40*, 3578.
(16) Winkel, L.; Berg, M.; Amini, M.; Hug, S. J.; Annette Johnson, C. Predicting groundwater arsenic contamination in Southeast Asia from surface parameters. *Nat. Geosci.* **2008**, *1*, 536−542.
(17) Podgorski, J. E.; Eqani, S. A. M. A. S.; Khanam, T.; Ullah, R.; Shen, H.; Berg, M. Extensive arsenic contamination in high-pH unconfined aquifers in the Indus Valley. *Sci. Adv.* **2017**, *3*, No. e1700935.
(18) Winkel, L. H. E.; Pham, T. K. T.; Lan, V. M.; Caroline, S.; Manouchehr, A.; Thi Ha, N.; Hung Viet, P.; Michael, B. Arsenic pollution of groundwater in Vietnam exacerbated by deep aquifer exploitation for more than a century. *Proc. Natl. Acad. Sci. U.S.A.* **2011**, *108*, 1246−1251.
(19) Rodríguez-Lado, L.; Sun, G.; Berg, M.; Zhang, Q.; Xue, H.; Zheng, Q.; Johnson, C. A. Groundwater arsenic contamination throughout China. *Science* **2013**, *341*, 866−868.
(20) Ayotte, J. D.; Medalie, L.; Qi, S. L.; Backer, L. C.; Nolan, B. T. Estimating the High-Arsenic Domestic-Well Population in the Conterminous United States. *Environ. Sci. Technol.* **2017**, *51*, 12443−12454.
(21) Yang, Q.; Jung, H. B.; Marvinney, R. G.; Culbertson, C. W.; Zheng, Y. Can arsenic occurrence rates in bedrock aquifers be predicted? *Environ. Sci. Technol.* **2012**, *46*, 2080−2087.
(22) Yang, N.; Winkel, L. H. E.; Johannesson, K. H. Predicting Geogenic Arsenic Contamination in Shallow Groundwater of South Louisiana, United States. *Environ. Sci. Technol.* **2014**, *48*, 5660−5666.
(23) Ayotte, J. D.; Nolan, B. T.; Gronberg, J. A. Predicting Arsenic in Drinking Water Wells of the Central Valley, California. *Environ. Sci. Technol.* **2016**, *50*, 7555−63.
(24) Zheng, Y.; Stute, M.; van Geen, A.; Gavrieli, I.; Dhar, R.; Simpson, H. J.; Schlosser, P.; Ahmed, K. M. Redox control of arsenic mobilization in Bangladesh groundwater. *Appl. Geochem.* **2004**, *19*, 201−214.
(25) Yang, Q.; Culbertson, C. W.; Nielsen, M. G.; Schalk, C. W.; Johnson, C. D.; Marvinney, R. G.; Stute, M.; Zheng, Y. J. S. oT. T. E. Flow and sorption controls of groundwater arsenic in individual boreholes from bedrock aquifers in central Maine, USA. *Sci.Total Environ.* **2015**, *505*, 1291−1307.
(26) Schreiber, M.; Simo, J.; Freiberg, P. J. H. J. Stratigraphic and geochemical controls on naturally occurring arsenic in groundwater eastern Wisconsin, USA. *Hydrogeol. J.* **2000**, *8*, 161−176.
(27) Ayotte, J. D.; Montgomery, D. L.; Flanagan, S. M.; Robinson, K. W. Arsenic in groundwater in eastern New England: occurrence, controls, and human health implications. *Environ. Sci. Technol.* **2003**, *37*, 2075−2083.
(28) Anawar, H. M.; Akai, J.; Komaki, K.; Terao, H.; Yoshioka, T.; Ishizuka, T.; Safiullah, S.; Kato, K. Geochemical occurrence of arsenic in groundwater of Bangladesh: sources and mobilization processes. *J. Geochem. Explor.* **2003**, *77*, 109−131.
(29) Ahmed, K. M.; Bhattacharya, P.; Hasan, M. A.; Akhter, S. H.; Alam, S. M. M.; Bhuyian, M. A. H.; Imam, M. B.; Khan, A. A.; Sracek, O. Arsenic enrichment in groundwater of the alluvial aquifers in Bangladesh: an overview. *Appl. Geochem.* **2004**, *19*, 181−200.
(30) Ravenscroft, P.; Burgess, W. G.; Ahmed, K. M.; Burren, M.; Perrin, J. Arsenic in groundwater of the Bengal Basin, Bangladesh: Distribution, field relations, and hydrogeological setting. *Hydrogeol. J.* **2005**, *13*, 727−751.
(31) Elith, J.; Leathwick, J. R.; Hastie, T. A working guide to boosted regression trees. *J. Anim. Ecol.* **2008**, *77*, 802−813.
(32) Prasad, A. M.; Iverson, L. R.; Liaw, A. Newer Classification and Regression Tree Techniques: Bagging and Random Forests for Ecological Prediction. *Ecosystems* **2006**, *9*, 181−199.
(33) Yu, W. H.; Harvey, C. M.; Harvey, C. F. Arsenic in groundwater in Bangladesh: A geostatistical and epidemiological framework for evaluating health effects and potential remedies. *Water Resour. Res.* **2003**, *39*, 1146−1151.
(34) Gelman, A.; Trevisani, M.; Lu, H.; Van Geen, A. Direct data manipulation for local decision analysis as applied to the problem of arsenic in drinking water from tube wells in Bangladesh. *Risk Anal.* **2004**, *24*, 1597−1612.
(35) Frederick, L.; VanDerslice, J.; Taddie, M.; Malecki, K.; Gregg, J.; Faust, N.; Johnson, W. P. Contrasting regional and national mechanisms for predicting elevated arsenic in private wells across the United States using classification and regression trees. *Water Res.* **2016**, *91*, 295−304.
(36) Hoque, M. A.; Burgess, W. G.; Ahmed, K. M. Integration of aquifer geology, groundwater flow and arsenic distribution in deltaic aquifers - A unifying concept. *Hydrol. Processes* **2017**, *31*, 2095−2109.
(37) Ravenscroft, P.; McArthur, J. M.; Rahman, M. S. J. H. P. Identifying multiple deep aquifers in the Bengal Basin: Implications for resource management. *Hydrol. Processes* **2018**, *32*, 3615−3632.
(38) Carr, J. R.; Mao, N.-h. A general form of probability kriging for estimation of the indicator and uniform transforms. *Math. Geol.* **1993**, *25*, 425−438.
(39) Gaus, I.; Kinniburgh, D.; Talbot, J.; Webster, R. Geostatistical analysis of arsenic concentration in groundwater in Bangladesh using disjunctive kriging. *Environ. Geol.* **2003**, *44*, 939−948.
(40) Ripley, B. D.; Venables, W. N. *Modern Applied Statistics with S*; Springer: New York, 2002; Vol. *537*.
(41) Anning, D. W.; Paul, A. P.; McKinney, T. S.; Huntington, J. M.; Bexfield, L. M.; Thiros, S. A. *Predicted Nitrate and Arsenic Concentrations in Basin-Fill Aquifers of the Southwestern United States*; US Department of the Interior, US Geological Survey, 2012.
(42) Friedman, J. H. Stochastic gradient boosting. *Comput. Stat. Data Anal.* **2002**, *38*, 367−378.
(43) Friedman, J. H. Greedy function approximation: a gradient boosting machine. *Ann. Math. Stat.* **2001**, 1189−1232.
(44) Breiman, L. Random forests. *Mach. Learn.* **2001**, *45*, 5−32.
(45) Greg, R., *gbm: Generalized Boosted Regression Models*. 2017.
(46) Andy, L.; Matthew, W. Classification and Regression by randomForest. *R. News* **2002**, *2*, 5.
(47) Max, K. *caret: Classification and Regression Training*. Astrophysics Source Code Library, 2018.
(48) Haibo, H.; Garcia, E. A. Learning from Imbalanced Data. *IEEE Transactions on Knowledge and Data Engineering* **2009**, *21*, 1263−1284.
(49) Shekhar, S.; Zhang, P.; Huang, Y. Spatial Data Mining. In *Data Mining and Knowledge Discovery Handbook*; Springer, 2009; pp 837−854.
(50) Roberts, D. R.; Bahn, V.; Ciuti, S.; Boyce, M. S.; Elith, J.; Guillera-Arroita, G.; Hauenstein, S.; Lahoz-Monfort, J. J.; Schröder, B.; Thuiller, W.; et al. Cross-validation strategies for data with

https://dx.doi.org/10.1021/acs.est.0c03617
Environ. Sci. Technol. 2020, 54, 9454−9463

temporal, spatial, hierarchical, or phylogenetic structure. *Ecography* **2017**, *40*, 913−929.

(51) Cho, K. H.; Sthiannopkao, S.; Pachepsky, Y. A.; Kim, K. W.; Kim, J. H. Prediction of contamination potential of groundwater arsenic in Cambodia, Laos, and Thailand using artificial neural network. *Water Res.* **2011**, *45*, 5535−44.

(52) Park, Y.; Ligaray, M.; Kim, Y. M.; Kim, J. H.; Cho, K. H.; Sthiannopkao, S. Development of enhanced groundwater arsenic prediction model using machine learning approaches in Southeast Asian countries. *Desalin. Water Treat.* **2016**, *57*, 12227−12236.

(53) Purkait, B.; Kadam, S. S.; Das, S. K. Application of Artificial Neural Network Model to Study Arsenic Contamination in Groundwater of Malda District, Eastern India. *J. Environ. Inf.* **2008**, *12*, 140−149.

(54) Chowdhury, M.; Alouani, A.; Hossain, F. Comparison of ordinary kriging and artificial neural network for spatial mapping of arsenic contamination of groundwater. *Stochastic Environ. Res. Risk Assess.* **2010**, *24*, 1−7.

(55) Lowers, H. A.; Breit, G. N.; Foster, A. L.; Whitney, J.; Yount, J.; Uddin, M. N.; Muneem, A. A. Arsenic incorporation into authigenic pyrite, Bengal Basin sediment, Bangladesh. *Geochim. Cosmochim. Acta* **2007**, *71*, 2699−2717.

(56) Zheng, Y.; van Geen, A.; Stute, M.; Dhar, R.; Mo, Z.; Cheng, Z.; Horneman, A.; Gavrieli, I.; Simpson, H.; Versteeg, R.; et al. Geochemical and hydrogeological contrasts between shallow and deeper aquifers in two villages of Araihazar, Bangladesh: Implications for deeper aquifers as drinking water sources. *Geochim. Cosmochim. Acta* **2005**, *69*, 5203−5218.

(57) Radloff, K. A.; Zheng, Y.; Michael, H. A.; Stute, M.; Bostick, B. C.; Mihajlov, I.; Bounds, M.; Huq, M. R.; Choudhury, I.; Rahman, M.; et al. Arsenic migration to deep groundwater in Bangladesh influenced by adsorption and water demand. *Nat. Geosci.* **2011**, *4*, 793−798.

(58) McArthur, J. M.; Banerjee, D. M.; Hudson-Edwards, K. A.; Mishra, R.; Purohit, R.; Ravenscroft, P.; Cronin, A.; Howarth, R. J.; Chatterjee, A.; Talukder, T.; et al. Natural organic matter in sedimentary basins and its relation to arsenic in anoxic ground water: the example of West Bengal and its worldwide implications. *Appl. Geochem.* **2004**, *19*, 1255−1293.

(59) McArthur, J. M.; Ravenscroft, P.; Banerjee, D. M.; Milsom, J.; Hudson-Edwards, K. A.; Sengupta, S.; Bristow, C.; Sarkar, A.; Tonkin, S.; Purohit, R. How paleosols influence groundwater flow and arsenic pollution: A model from the Bengal Basin and its worldwide implication. *Water Resour. Res.* **2008**, *44*, No. W11411.

(60) Hoque, M. A.; Burgess, W. G.; Shamsudduha, M.; Ahmed, K. M. Delineating low-arsenic groundwater environments in the Bengal Aquifer System, Bangladesh. *Appl. Geochem.* **2011**, *26*, 614−623.

(61) Umitsu, M. Late quaternary sedimentary environments and landforms in the Ganges Delta. *Sediment. Geol.* **1993**, *83*, 177−186.

(62) Goodbred, S. L., Jr; Kuehl, S. A.; Steckler, M. S.; Sarker, M. H. Controls on facies distribution and stratigraphic preservation in the Ganges−Brahmaputra delta sequence. *Sediment. Geol.* **2003**, *155*, 301−316.

(63) Sincavage, R.; Goodbred, S.; Pickering, J. Holocene Brahmaputra River path selection and variable sediment bypass as indicators of fluctuating hydrologic and climate conditions in Sylhet Basin, Bangladesh. *Basin Res.* **2018**, *30*, 302−320.

(64) Harvey, C. F.; Swartz, C. H.; Badruzzaman, A. B. M.; Keon-Blute, N.; Yu, W.; Ali, M. A.; Jay, J.; Beckie, R.; Niedan, V.; Brabander, D.; Oates, P. M.; Ashfaque, K. N.; Islam, S.; Hemond, H. F.; Ahmed, M. F. Arsenic mobility and groundwater extraction in Bangladesh. *Science* **2002**, *298*, 1602−1606.

(65) Stute, M.; Zheng, Y.; Schlosser, P.; Horneman, A.; Dhar, R. K.; Datta, S.; Hoque, M. A.; Seddique, A. A.; Shamsudduha, M.; Ahmed, K. M.; van Geen, A. Hydrological control of As concentrations in Bangladesh groundwater. *Water Resour. Res.* **2007**, *43*, No. W09417.

(66) Polizzotto, M. L.; Harvey, C. F.; Sutton, S. R.; Fendorf, S. Processes conducive to the release and transport of arsenic into aquifers of Bangladesh. *Proc. Natl. Acad. Sci. U.S.A.* **2005**, *102*, 18819−18823.

(67) Mladenov, N.; Zheng, Y.; Simone, B.; Bilinski, T. M.; McKnight, D. M.; Nemergut, D.; Radloff, K. A.; Rahman, M. M.; Ahmed, K. M. Dissolved Organic Matter Quality in a Shallow Aquifer of Bangladesh: Implications for Arsenic Mobility. *Environ. Sci. Technol.* **2015**, *49*, 10815−10824.

(68) McArthur, J. M.; Ravenscroft, P.; Safiulla, S.; Thirlwall, M. F. Arsenic in groundwater: Testing pollution mechanisms for sedimentary aquifers in Bangladesh. *Water Resour. Res.* **2001**, *37*, 109−117.

(69) Ravenscroft, P.; Mcarthur, J.; Hoque, B. Geochemical and palaeohydrological controls on pollution of groundwater by arsenic. In *Arsenic Exposure and Health Effects IV*; Elsevier Science Ltd., 2001.

(70) Wang, Y.; Pi, K.; Fendorf, S.; Deng, Y.; Xie, X. Sedimentogenesis and hydrobiogeochemistry of high arsenic Late Pleistocene-Holocene aquifer systems. *Earth-Sci. Rev.* **2019**, *189*, 79−98.

(71) O'reilly, S.; Strawn, D.; Sparks, D. Residence time effects on arsenate adsorption/desorption mechanisms on goethite. *Soil Sci. Soc. Am. J.* **2001**, *65*, 67−77.

(72) Sun, X.; Doner, H. E. An investigation of arsenate and arsenite bonding structures on goethite by FTIR. *Soil Sci.* **1996**, *161*, 865−872.

(73) Fendorf, S.; Eick, M. J.; Grossl, P.; Sparks, D. L. Arsenate and chromate retention mechanisms on goethite. 1 Surface structure. *Environ. Sci. Technol.* **1997**, *31*, 315−320.

(74) Manning, B. A.; Fendorf, S. E.; Goldberg, S. Surface structures and stability of arsenic (III) on goethite: spectroscopic evidence for inner-sphere complexes. *Environ. Sci. Technol.* **1998**, *32*, 2383−2388.

(75) Aziz, Z.; Bostick, B. C.; Zheng, Y.; Huq, M. R.; Rahman, M. M.; Ahmed, K. M.; Geen, A. V. Evidence of decoupling between arsenic and phosphate in shallow groundwater of Bangladesh and potential implications. *Appl. Geochem.* **2017**, *77*, 167.

(76) Dhar, R. K.; Zheng, Y.; Stute, M.; Geen, A. V.; Cheng, Z.; Shanewaz, M.; Shamsudduha, M.; Hoque, M. A.; Rahman, M. W.; Ahmed, K. M. Temporal variability of groundwater chemistry in shallow and deep aquifers of Araihazar, Bangladesh. *J. Contam. Hydrol.* **2008**, *99*, 97−111.

(77) Goodbred, S.; Paola, P. M.; Ullah, M. S.; Pate, R.; Khan, S. R.; Kuehl, S.; Singh, S. K.; Rahaman, W. Piecing together the Ganges-Brahmaputra-Meghna River delta: Use of sediment provenance to reconstruct the history and interaction of multiple fluvial systems during Holocene delta evolution. *Geol. Soc. Am. Bull.* **2014**, *126*, 1495−1510.

(78) Thompson, L. G.; Yao, T.; Davis, M.; Henderson, K.; Mosley-Thompson, E.; Lin, P.-N.; Beer, J.; Synal, H.-A.; Cole-Dai, J.; Bolzan, J. Tropical climate instability: The last glacial cycle from a Qinghai-Tibetan ice core. *Science* **1997**, *276*, 1821−1825.

(79) Gasse, F.; Arnold, M.; Fontes, J. C.; Fort, M.; Gibert, E.; Huc, A.; Bingyan, L.; Yuanfang, L.; Qing, L.; Melieres, F.; et al. A 13,000-year climate record from western Tibet. *Nature* **1991**, *353*, 742−745.

(80) Goodbred, S., Jr; Kuehl, S. A. The significance of large sediment supply, active tectonism, and eustasy on margin sequence development: Late Quaternary stratigraphy and evolution of the Ganges−Brahmaputra delta. *Sediment. Geol.* **2000**, *133*, 227−248.

(81) Besancon, J.; Islam, S.; Hemond, H. F.; Harvey, C. Mobility of arsenic in a Bangladesh aquifer: Inferences from geochemical profiles, leaching data, and mineralogical characterization. *Geochim. Cosmochim. Acta* **2004**, *68*, 4539−4557.

(82) Horneman, A.; van Geen, A.; Kent, D. V.; Mathe, P.; Zheng, Y.; Dhar, R.; O'connell, S.; Hoque, M.; Aziz, Z.; Shamsudduha, M.; et al. Decoupling of As and Fe release to Bangladesh groundwater under reducing conditions. Part I: Evidence from sediment profiles. *Geochim. Cosmochim. Acta* **2004**, *68*, 3459−3473.

(83) Van Geen, A.; Rose, J.; Thoral, S.; Garnier, J.; Zheng, Y.; Bottero, J. Decoupling of As and Fe release to Bangladesh groundwater under reducing conditions. Part II: Evidence from sediment incubations. *Geochim. Cosmochim. Acta* **2004**, *68*, 3475−3486.

(84) Sun, J.; Chillrud, S. N.; Mailloux, B. J.; Bostick, B. C. In situ magnetite formation and long-term arsenic immobilization under

advective flow conditions. *Environ. Sci. Technol.* **2016**, *50*, 10162−10171.

https://dx.doi.org/10.1021/acs.est.0c03617
Environ. Sci. Technol. 2020, 54, 9454−9463